

Case Report

Pediatric focally pigmented choroidal melanoma: Imaging with pathological correlation

Paolo Galluzzi^a, Rossella Occhini^b, Alfonso Cerase^{a,*}, Paolo Toti^b, Theodora Hadjistilianou^c, Carlo Venturi^a and Sonia De Francesco^c

^a*Unit of Neuroimaging and Neurointervention (NINT), Department of Neurological and Sensorineural Sciences, Azienda Ospedaliera Universitaria Senese, Siena, Italy*

^b*Section of Pathology, Department of Human Pathology and Oncology, University of Siena, Siena, Italy*

^c*Unit of Ophthalmology, and Retinoblastoma Referral Center, Department of Neurological and Sensorineural Sciences, Azienda Ospedaliera Universitaria Senese, Siena, Italy*

Received 16 June 2011

Revised 8 November 2011

Accepted 23 January 2012

Abstract. We report a 9-year-old-boy with no predisposing factors who presented with left eye leukocoria from a complete retinal detachment at ophthalmoscopy. Imaging showed an intraocular dome-shaped mass of low to moderate internal reflectivity at ultrasound, low T2-weighted signal intensity, lack of T1-weighted high signal intensity, and subtle gadolinium-enhancement at magnetic resonance imaging, and lack of calcifications at computed tomography. Due to the rapid extensive intraocular growth, the affected eye was enucleated. Pathologic examination showed a choroidal melanoma with only focal pigmentation. Despite its very rare incidence in the pediatric population, choroidal melanoma should be included in the differential diagnosis of leukocoria.

Keywords: Choroidal malignant melanoma, computed tomography, focal pigmentation, magnetic resonance imaging, pediatric ocular malignancy

1. Introduction

Choroidal malignant melanoma is extremely rare in childhood, with only 0.6 to 1.6% of affected patients under 20 yr of age [1–5]. The purpose of this case report is to increase awareness to choroidal malignant melanoma

in childhood, by presenting clinical, neuroimaging, and pathologic findings of a focally pigmented one occurring in a 9-year-old boy.

2. Case report

A 9-year-old-boy was referred to the Retinoblastoma Referral Center of our institution because of leukocoria and exotropia in his left eye. Three months before, in another institution magnetic resonance imaging (MRI) had showed an intraocular dome-shaped mass in the left

*Corresponding author: Alfonso Cerase, Unit of Neuroimaging and Neurointervention - NINT, Department of Neurological and Sensorineural Sciences, Azienda Ospedaliera Universitaria Senese, Policlinico "Santa Maria alle Scotte", Viale Mario Bracci, 16 53100 Siena, Italy. Tel.: +39 0577 585040/4; Fax: +39 0577 586197; E-mail: alfonsocerase@gmail.com.

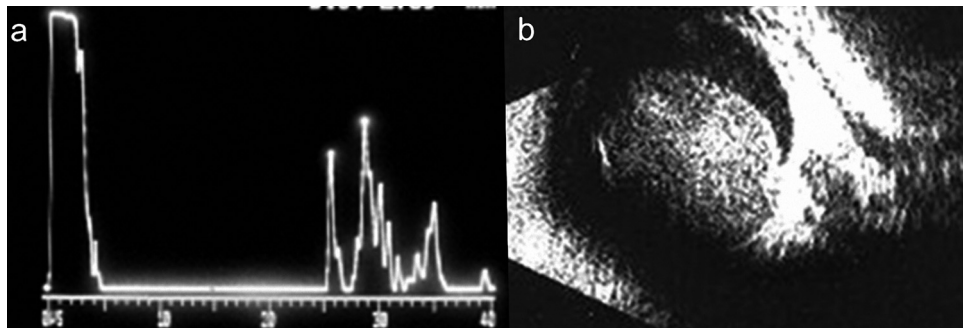


Fig. 1. Ultrasound. A-scan (a) shows a moderate to low internal reflectivity of the intraocular mass. B-scan (b) shows its dome-like configuration, retinal detachment, and cloudy vitreous.

eye, associated with a complete exudative retinal detachment. At admission, this patient had no detectable vision in the left eye. At slit-lamp examination, leukocoria had resulted from an old total retinal exudative detachment. The retina was thickened and presented cirrhotic arterial vessels with microaneurysms, especially in the nasal periphery. No pigmentary changes were observed. History revealed that a transient left exophoria had been observed by patient's parents three years before. Ultrasound confirmed the total retinal detachment and showed a smooth, moderate- to low-reflectivity dome-shaped intraocular mass lesion associated with a cloudy vitreous (Fig. 1). MRI of the orbits confirmed the dome-shaped lesion in the left eye, growing behind the retinal layers, which appeared anteriorly dislocated, and associated with signs of chronic hemorrhagic total retinal detachment (Figs. 2a–2e). On T1-weighted axial images, the lesion showed a very slight high-intensity signal when compared to the contralateral vitreous. On T2-weighted images, the lesion showed a clear-cut low-intensity signal in comparison with the contralateral vitreous. On both T1- and T2-weighted images, the mass showed the same intensity signal when compared to the extraocular muscles. There were some signal voids in the lesion periphery and in the detached retina, consistent with hemosiderosis. Gadolinium-enhanced unsubtracted and subtracted T1-weighted images showed a moderate enhancement of the lesion, as well as the detached retina. There was no evidence of any other primary or metastatic intracranial lesions. Computed tomography (CT) scan confirmed the lack of calcifications (Fig. 2f). One week later, B-mode scan showed a clear-cut growth of the mass, leading to enucleation of the left eye and insertion of a 20 mm hydroxyapatite implant. After surgery, the globe was immersion-fixed (72 h) in 10% buffered formalin. At the opening of the globe,

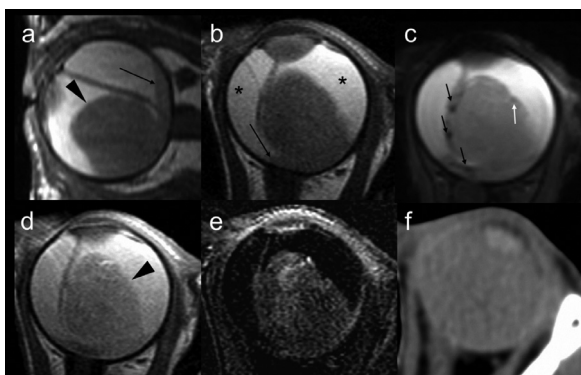


Fig. 2. Unenhanced sagittal T2-weighted (a), and axial T1- (b) and T2*-weighted (c), and axial gadolinium-enhanced nonsubtracted (d) and subtracted (e) T1-weighted magnetic resonance images obtained by a surface coil confirm the dome-shaped mass lesion (arrowheads) in the inferotemporal quadrant of the left eye, growing behind the retinal layers. The associated complete retinal detachment is associated with a subretinal exudate of high-intensity signal on T1-weighted images (asterisks), fluid-fluid level (long black arrows), and focal signal voids consistent with hemosiderosis (short black arrows). The mass lesion shows slight high-intensity signal on T1-weighted images when compared to the contralateral vitreous (not shown), low-intensity signal on T2-, and T2*-weighted images, a focal signal voids consistent with hemosiderosis (white arrow), and slight gadolinium-enhancement. At unenhanced axial computed tomography image (f), the lesion shows high attenuation density, undistinguishable from the retinal exudate, and confirms the lack of intraocular calcifications.

a whitish large mass was present at the posterior pole. The retina was raised and completely detached by a large mass, showing a domed shape, measuring 12 mm width and 12 mm thickness. At histology (Fig. 3), the mass was constituted by spindle, cohesive cells with poorly defined cell borders. Necrosis was absent. Pigmentation was focally present. Spindle nuclei either showed nuclear folds appearing dark stripes parallel to the long axis of the nuclei (due to enfolding of the

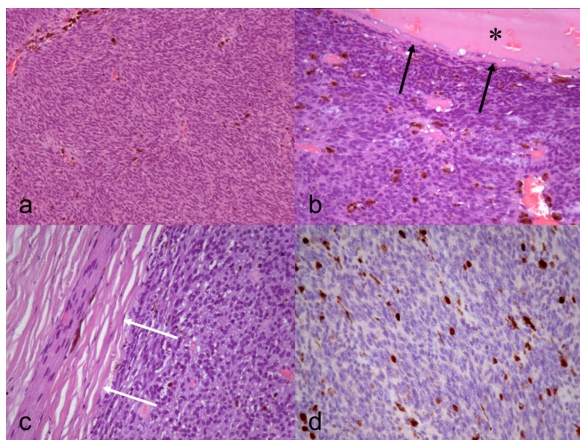


Fig. 3. Histology shows a spindle cell choroidal malignant melanoma comprised of a syncytium of spindle A and B cells with oval nuclei and distinct nucleoli, poor in melanin pigmentation (a, b, c, Hematoxylin-Eosin; original magnification, 10×). The Bruch's membrane is not trespassed (black arrows). The asterisk marks the hemorrhagic subretinal exudate. There is minimal early scleral invasion (white arrows). A non-infiltrated penetrating nerve (arrowhead) is evident inside the sclera. The lesion had a low proliferative index, i.e. mitoses <1 per 10 high power field. The proliferation index (Ki67/MIB-1) was <5% (d).

nucleus, as apparent in the cross section), or with prominent nucleoli (according to the Callender classification, spindle A and spindle B cells, respectively). No epithelioid cells were identified, i.e. large polygonal cell with defined cell border and plump nucleus with prominent nucleolus. Mitoses were present, yet they were extremely rare, below 1×10 high power field. Neoplastic mass involved the choroid but did not infiltrate the Bruch's membrane and minimally infiltrated the sclera. The main morphologic feature indicating malignant melanoma was the large volume of the mass, along with neoplastic infiltration of the sclera. Immunohistochemistry showed cytoplasm positivity for HMB45, melan-A, microphthalmia associated transcription factor and S-100 protein, negativity for cytokeratins, glio-fibrillary acidic protein, neuron specific enolase. Cell growth fraction, identified by Ki67 labeling, was less than 5%. These morphological and immunocytochemical features were consistent with a proliferative melanocytic lesion. Final diagnosis was scarcely pigmented choroidal malignant melanoma, spindle A and B mixed type.

The child did not undergo other therapies, and underwent a close pediatric and ocular oncology follow-up. Four years later, there was no evidence of local relapse or systemic dissemination.

3. Discussion

Choroidal malignant melanoma is extremely rare in children [1–5]. Only several single cases have been described, with little information regarding the long-term prognosis. In the first decade of life, the incidence is very low, and may account for 0.11% to 0.12% of cases. The tumor is usually unilateral, and no gender difference has been observed. Associated hemorrhagic detachment is rare [6]. Choroidal malignant melanoma may be associated with pre-existing conditions such as oculo-dermal melanocytosis, familial atypical mole-melanoma, Li-Fraumeni syndrome, familial uveal melanocytoma, neurofibromatosis type 1, dysplastic nevus syndrome, cutaneous melanoma, and immunosuppression, however it can be also sporadic and/or influenced by hormonal changes occurring in puberty [4,5]. The patient reported herein did not present with any of these conditions. The developments in the genetics of melanoma [7–9] including monosomy 3 and guanine nucleotide-binding protein subunit alpha-11 mutations will be very useful in disease classification. Treatment options for high-risk uveal malignant melanomas remain radiotherapy and enucleation.

In the pediatric age, the differential diagnosis for leukocoria includes late retinoblastoma, benign nevus, melanocytoma, intraocular metastasis, Coats' disease, neuroepithelial cysts, hemangiomas, hematomas and acquired inflammatory masses [10–14].

The patient reported herein was referred to our institution with the differential diagnosis between late onset retinoblastoma or Coats' disease. Clinical and ophthalmoscopic diagnosis was very challenging. Despite the presence of leukocoria and anomalous vessels, the patient's age was very atypical for both retinoblastoma and Coats' disease, and there was lack of pigmentary changes at fundus examination. Ultrasound showed a medium- to low-reflectivity dome-shaped intraocular mass associated with a cloudy vitreous. A definitive diagnosis of melanoma was not proposed because of its rarity in the pediatric age, and the absence of pigmentation at ophthalmoscopy. MRI and CT were performed. MRI confirmed a lesion growing behind the retina, i.e. a choroidal tumor. At MRI, choroidal malignant melanoma usually shows a markedly high-intensity signal on unenhanced T1-weighted images and low-intensity signal on T2-weighted images when compared with contralateral vitreous. This results from the high content of paramagnetic melanin, which shortens both T1 and T2 relaxation times. Rarely, choroidal malignant melanoma shows T2 isointensity [13]. In the patient

reported herein, the lesion showed only a very slight high-intensity signal on T1-weighted images, and low-intensity signal on T2-weighted images. Additionally, it was isointense to the extraocular muscles. This pattern has been described only in another single case of scarcely pigmented choroidal malignant melanoma in childhood [2]. Thus, the signal intensity could not differentiate scarcely pigmented melanoma from retinoblastoma. There were no intralesional signal voids consistent for calcifications [15], and this was confirmed by both CT and histology. Retinoblastoma usually calcifies, however diffuse infiltrative type usually does not calcify and thus could not be totally ruled out [16]. The high intensity signal of the retinal exudate on both T1- and T2-weighted images, lack of intraocular calcification, and contrast-enhancement of the detached retina could suggest the diagnosis of Coats' disease [10–12, 14]. However, the presence of an intraocular mass, as well as its homogeneous gadolinium-enhancement, reduced the probability of Coats' disease, whose contrast enhancement is usually limited to detached retinal layers. Moreover, in Coats' disease and retinoblastoma the affected globe may be smaller than the contralateral normal globe [17,18], and this did not occur in the patient reported herein. Additionally, the only moderate gadolinium-enhancement made unlikely the possibility of strongly gadolinium-enhancing lesions such as medulloepithelioma, hemangioma and leiomyoma [19–22]. A possible explanation for the moderate gadolinium-enhancement is the lack of extracellular space of packed spindle cells. Finally, choroidal metastases from solid tumors may present with a dome-shaped morphology and high-intensity signal on T1-weighted images, low-intensity signal on T2-weighted images, and gadolinium-enhancement, however these are typically seen in adulthood [23].

Histopathology documented a very large tumor, spindle cell type, minimally infiltrating the sclera and without infiltration of the retina, with low mitotic index, low proliferative index, and no necrosis. Benign nevus was excluded due to the dimensions of the mass, the relatively high proliferative index, and cellular morphology. Magnocellular nevus, or melanocytoma, is usually smaller, deeply pigmented and composed of large polygonal epithelioid cells. Schwannoma, leiomyoma, neurofibroma, meningioma and fibrous histiocytoma were excluded on the basis of morphological findings. The morphological characteristics seemed to indicate an excellent prognosis, however a benign counterpart of melanoma does not exist [24,25].

In conclusion, in this uncommon and misleading case, ophthalmoscopy was unable to solve the differential

diagnosis challenge due to the absence of pigmentation, and ultrasound did not suspect a choroidal malignant melanoma due to the rarity of this entity in the pediatric age. The correct diagnosis might have been suggested by the association of MRI and CT findings, including the lack of calcifications, the high-intensity signal on T1-weighted MRI images albeit very slight, and the only moderate gadolinium-enhancement. The differential diagnosis of choroidal tumors of the pediatric age has to include melanoma.

Acknowledgements

We thank AIGR Associazione Italiana Genitori Retinoblastoma ONLUS.

We thank Roberto Falieri from the Library of the School of Medicine, University of Siena, Policlinico "Santa Maria alle Scotte", Siena, Italy, for his great help in searching pertinent references for this manuscript.

References

- [1] Cury D, Lucic H, Irvine AR Jr. Prepuberal intraocular malignant melanoma. Am J Ophthalmol 1959;47(5, Part 2):202–6.
- [2] Meyer D, Yoser S, Xu S, Westmoreland D. Amelanotic malignant choroidal melanoma in a 10-year-old girl. J Pediatr Ophthalmol Strabismus 2000;37(6):365–8.
- [3] Singh AD, Shields CL, Shields JA, Sato T. Uveal melanoma in young patients. Arch Ophthalmol 2000;118(7):918–23.
- [4] Soni S, Lee DS, DiVito J Jr, Bui AH, DeRaffele G, Radel E, et al. Treatment of pediatric ocular melanoma with high-dose interleukin-2 and thalidomide. J Pediatr Hematol Oncol 2002;24(6):488–91.
- [5] Shields JA, Narsipuri SS, Shields CL, Sperber DE. Choroidal melanoma in an immunosuppressed child with minimal change nephrotic syndrome. Retina 2004;24(3):454–5.
- [6] Puri P, Gupta M, Rundle PA, Rennie IG. Choroidal melanoma presenting as a haemorrhagic detachment in a 12-year old. Eye (Lond) 2003;17(3):425–7.
- [7] Herlyn M, Nathanson KL. Taking the guesswork out of uveal melanoma. N Engl J Med 2010;363(23):2256–7.
- [8] Scolyer RA, Long GV, Thompson JF. Evolving concepts in melanoma classification and their relevance to multidisciplinary melanoma patient care. Mol Oncol 2011;5(2):124–36.
- [9] Romano E, Schwartz GK, Chapman PB, Wolchock JD, Carvajal RD. Treatment implications of the emerging molecular classification system for melanoma. Lancet Oncol 2011; 12(9):913–22.
- [10] Mafee MF, Goldberg MF, Greenwald MJ, Schulman J, Malmed A, Flanders AE. Retinoblastoma and simulating lesions: role of CT and MR imaging. Radiol Clin North Am 1987;25(4):667–82.
- [11] Mafee MF, Goldberg MF, Cohen SB, Gotsis ED, Safran M, Chekuri L, et al. Magnetic resonance imaging versus computed tomography of leukocoric eyes and use of in vitro proton magnetic resonance spectroscopy of retinoblastoma. Ophthalmology 1989;96(7):965–75.

- [12] Smirniotopoulos JG, Bargallo N, Mafee MF. Differential diagnosis of leukokoria: radiologic-pathologic correlation. *Radiographics* 1994;14(5):1059–79.
- [13] De Potter P, Shields JA, Shields CL. Tumors of the uvea. In: De Potter P, Shields JA, Shields CL, editors. *MRI of the eye and orbit*. J.B. Philadelphia: Lippincott Company; 1995, p. 55–9.
- [14] Edward DP, Mafee MF, Garcia-Valenzuela E, Weiss RA. Coats' disease and persistent hyperplastic primary vitreous. Role of MR imaging and CT. *Radiol Clin North Am* 1998; 36(6):1119–31.
- [15] Galluzzi P, Hadjistilianou T, Cerase A, De Francesco S, Toti P, Venturi C. Is CT still useful in the study protocol of retinoblastoma? *AJNR Am J Neuroradiol* 2009;30(9):1760–5.
- [16] Brisse HJ, Lumbroso L, Fréneaux PC, Validire P, Doz FP, Quintana EJ, et al. Sonographic, CT, and MR imaging findings in diffuse infiltrative retinoblastoma: report of two cases with histologic comparison. *AJNR Am J Neuroradiol* 2001;22(3): 499–504.
- [17] Galluzzi P, Venturi C, Cerase A, Vallone IM, Bracco S, Bardelli AM, et al. Coats disease: smaller volume of the affected globe. *Radiology* 2001;221(1):64–9.
- [18] de Graaf P, Knol DL, Moll AC, Imhof SM, Schouten-van Meeteren AY, Castelijns JA. Eye size in retinoblastoma: MR imaging measurements in normal and affected eyes. *Radiology* 2007;244(1):273–80.
- [19] Mashayekhi A, Shields CL. Circumscribed choroidal hemangioma. *Curr Opin Ophthalmol* 2003;14(3):142–9.
- [20] Oh KJ, Kwon BJ, Han MH, Hwang PG, Kim CJ, Na DG, et al. MR imaging findings of uveal leiomyoma: three cases. *AJNR Am J Neuroradiol* 2005;26(1):100–3.
- [21] Singh AD, Kaiser PK, Sears JE. Choroidal hemangioma. *Ophthalmol Clin North Am* 2005;18(1):151–61.
- [22] Cerase A, De Francesco S, Citterio A, Hadjistilianou T, Malandrini A, Mastrangelo D, et al. Growth of congenital malignant teratoid medulloepithelioma of the ciliary body: a case study. *J Neurooncol* 2010;96(3):443–8.
- [23] Lemke AJ, Hosten N, Wiegel T, Prinz RD, Richter M, Bechrakis NE, et al. Intraocular metastases: differential diagnosis from uveal melanomas with high-resolution MRI using a surface coil. *Eur Radiol* 2001;11(12):2593–601.
- [24] Font RL, Croatto JO, Rao NA. *Tumors of the eye and ocular adnexa*. Washington: Armed Forces Institute of Pathology; 2006.
- [25] Yanoff M, Sassani JW. *Ocular pathology*. 6th ed. Amsterdam: Mosby Elsevier; 2009.